Energy absorption performance of steel tubes enhanced by a nanoporous material functionalized liquid

Xi Chen
Department of Civil Engineering and Engineering Mechanics, Columbia University, New York, New York 10027-6699

Falgun B. Surani and Xinguo Kong
Department of Civil Engineering, University of Akron, Akron, Ohio 44325-3905

Venkata K. Punyamurtula and Yu Qiao[a)]
Department of Structural Engineering, University of California at San Diego, La Jolla, California 92093-0085

(Received 4 July 2006; accepted 12 November 2006; published online 14 December 2006)

The compressive behaviors of steel cells enhanced by a nanoporous silica functionalized liquid are investigated. As the empty space in the ductile cell is filled by an aqueous suspension of hydrophobic nanoporous silica gel, the work done by the compressive load along the axial direction can be dissipated not only through the ordinary cell-wall buckling but also via the extended yielding and the pressure-induced infiltration. As a result, the energy absorption efficiency, either on mass or on volumetric basis, is considerably improved. © *2006 American Institute of Physics*.
[DOI: 10.1063/1.2405852]

Developing advanced energy absorption materials and structures (EAMS) is of both fundamental scientific interest and great technological importance. As an EAMS is subjected to external loadings, the associated kinetic and strain energies can be converted, often irreversibly, to other forms, such as heat,[1] electricity,[2] surface/interface tension,[3–6] etc., based on which protection or damping devices, e.g., car bumpers, soldier armors, and blast resistant layers, can be designed.

Due to its high energy absorption efficiency, cellular structure is one of the most attractive EAMS. Commonly used cellular structures include space filling foams and their two-dimensional counterparts, honeycombs, which are lightweight and can be made with relative ease by all major material categories.[7] In these materials, performance is optimized by geometric arrangement of the solids in space to form interconnected or isolated cells. When compressive loadings are applied, the cell walls can buckle, which is the primary energy absorption mechanism. They are widely applied for shock mitigation, packaging, as well as damping. Comprehensive reviews of cellular structures have been given by a number of researchers.[8–10]

Honeycomb is one of the most widely applied cellular structures. When being compressed from the lateral direction, the cell walls can deform quite smoothly. However, if the compressive load is applied along the out-of-plane direction, during the buckling process the working load is highly nonuniform. Under this condition, especially in a thin-walled structure, the wavelengths of wrinkles in cell walls are much smaller than the structural size. Initially, as the cell wall is nearly perfect, buckling initiation demands a large stress. As the cell wall becomes locally sigmoidal, the critical stress for the expansion of wrinkled zone becomes much lower. That is, while the cell-wall buckling is activated at a high stress level, the major portion of the energy absorbing process, which dominates the overall energy absorption efficiency, takes place at a relatively low stress level, significantly lowering the overall protection/damping capacity.

One method to solve this problem is to reinforce the honeycomb by a filler, particularly, a liquid filler. The mechanical property of liquid-containing cellular structures has been an active research area.[11] Usually, compared with the network material, the liquid is of a relatively low weight density, and thus the structure is still lightweight. Moreover, the liquid can spontaneously fit well with the cell wall, avoiding possible problems of filler-network mismatch. The thermal, electrical, and magnetic properties of the structure can also be adjusted in broad ranges. However, since most of liquids are nearly incompressible and therefore cannot accommodate cell-wall buckling, the liquid filled honeycombs are often rigid; that is, the major advantage of being cellular is lost.

Recently, through a series of pressure induced infiltration experiments,[3–6,12–14] an energy absorbing, nanoporous material functionalized (NMF) liquid was developed. The system is formed by immersing a lyophobic nanoporous material in a liquid. Due to the capillary effect, the liquid can enter the nanopores only when a sufficiently high pressure is applied. Under the high pressure, as the large nanopore surface is exposed to the infiltrated liquid molecules, a significant portion of the external work is converted to the solid-liquid

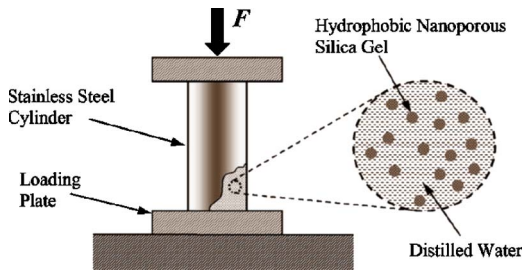

FIG. 1. (Color online) Schematic diagram of the experimental setup.

[a)]Author to whom correspondence should be addressed; electronic mail: yqiao@ucsd.edu

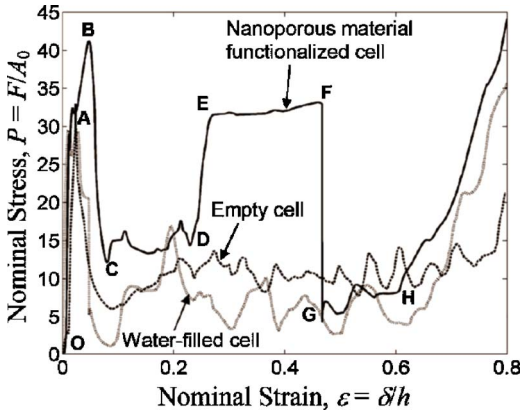

FIG. 2. (Color online) Typical stress-strain curves.

interfacial tension, which, since the infiltration process is irreversible, is effectively dissipated, leading to a high energy absorption efficiency at the level of 10–100 J/g.

A major concern of using NMF liquids to enhance honeycombs is related to the pressure difference across the cell wall. In the interior of a honeycomb panel, since the NMF liquid is compressible and the pressure is balanced by adjacent cells, the buckling behavior should be quite similar with that of empty ones. At the lateral surface of the panel, however, the large pressure difference can be high. If these cells buckle and fail easily, the overall energy absorption capacity would be relatively low.

In order to validate the concept of NMF liquid filled honeycombs, particularly to analyze the behaviors of cells at outer surfaces, the experimental setup depicted in Fig. 1 was developed. The testing system consisted of a thin-walled stainless steel cylinder and a liquid phase sealed in it. The height, outer diameter, and wall thickness of the cylinder were $h=25.4$ mm, $2R=6.86$ mm, and $t=0.13$ mm, respectively. Both ends of the cell were fixed on stainless steel loading plates using a J-B Weld epoxy glue. The cell was filled by an aqueous suspension of 0.4 g of Fluka 100 C_8 reversed phase nanoporous silica gel. The sample preparation was performed under water so that no air was entrapped. The nanoporous silica gel was hydrophobic. The average nanopore size was 7.8 nm. The specific nanopore volume was 0.55 cm^3/g. At the infiltration pressure of about 18 MPa, 1 g of the silica gel can dissipate about 14 J of energy. The details of the NMF liquid behavior have been documented elsewhere.[3,4]

The samples were tested using a type 5569 Instron machine. The crosshead speed was set to 0.5 mm/min. For comparison purpose, empty cells and cells filled by distilled water were also tested. For each type of cell, three to five samples were analyzed. Figure 2 shows typical stress-strain curves, where the nominal stress is defined as $P=F/A_0$, and the nominal strain is defined as $\varepsilon=\delta/h$, with F being the applied load, δ the piston displacement, and $A_0=36.9$ mm^2 the cross-sectional area of the steel cell.

It can be seen clearly that the deformability of the empty cell is quite high. After the initial linear compression stage, as the buckling initiates and continues, a broad plateau is formed, with the width of more than 70% of the initial cell height. As discussed above, due to the change in cell-wall configuration, the buckling initiation stress is much higher than the buckling development stress. The buckling plateau is quite jerky, consisting of a number of "bumps." Each bump reflects the stress accumulation, formation, and folding process of a wrinkle.

As the cell is filled by distilled water, since the compressibility of water is negligible, the cell-wall buckling is suppressed, and initially the energy dissipation is dominated by the extended cell wall yielding along the radius direction. As a result, the system becomes quite rigid, and shortly after the peak load is reached, the inner pressure becomes sufficiently high such that abrupt cracking takes place along the longitudinal direction. After the liquid leaks, the system behavior resembles that of an empty cell, except that, since the crack weakens the cell wall, the buckling of the fractured cell occurs at a relatively low stress level. Depending on the crack length, the decrease in buckling stress is in the range of 5%–25%. Therefore, the energy absorption capacity is reduced, as shown in Table I, where the absorbed energy U is calculated as the average area under the load-displacement curves in the nominal strain range of 0–0.75, and m and V are the system mass and the system volume, respectively.

The solid curve in Fig. 2 indicates the behavior of a cell filled by the NMF liquid. After the initial linear compression section (OA), as the critical nominal stress of about 35 MPa is reached the cell wall deforms plastically along the radius direction, since the buckling is suppressed by the liquid phase. As the cell is compressed, the pressure increases continuously. Eventually, at point B, the pressure induced infiltration in the largest nanopores is activated and the liquid phase becomes highly compressible. As a result, buckling takes place. As a major wrinkle is formed, the stress quickly drops to C. In the NMF cell, because the cell wall is supported by the liquid phase, the buckling can occur only outward, leading to a sudden increase in system volume, ΔV, and thus the cell becomes only partly filled. Under this condition, the system behavior is similar to that of an empty cell, until the cell is compressed to point D and ΔV is "consumed" by wrinkle folding.

As the liquid phase starts to carry load again, the nominal stress increases from D to E. When P rises to 32 MPa, the pressure induced infiltration is reactivated, forming the second plateau EF. As the plastic strain in cell wall is increasingly large, abrupt cracking occurs at point F, somewhat similar with the failure observed in the water-filled cell. The total system volume change associated with the second

TABLE I. Comparison of empty, water-filled, and NMF liquid enhanced cells.

	Mass m (g)	Volume V (cm^3)	Absorbed energy (J)	U/m (J/g)	U/V (J/cm^3)
Empty cell	0.57	0.94	6.54	11.5	6.96
Water-filled cell	1.48	0.94	5.80	3.92	6.17
NMF liquid enhanced Cell	1.20	0.94	16.7	13.9	17.8

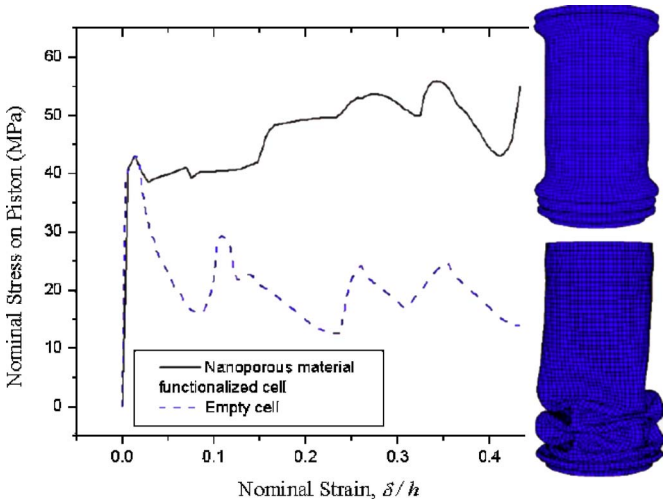

FIG. 3. (Color online) Finite element simulation of the empty and the NFM liquid enhanced cells.

loading is about 170 mm^3, smaller than the total nanopore volume; that is, the energy absorption capacity of the nanoporous silica gel is not fully utilized. As the cell becomes empty, the nominal stress drops to 7 MPa, after which the system behavior is similar to that of an empty cell (section *GH*). According to Table I, compared with the energy absorption efficiency of an empty cell, U/m of the NMF liquid filled cell is more than 20% larger and U/V is more than two times higher.

In order to gain more insights into the buckling mechanism, finite element simulations were carried out for both empty and NFM-liquid-filled steel tubes by using ABAQUS. The geometry, the Young's modulus (190 GPa), the yield stress (520 MPa), and the strain hardening exponent (0.4) of the tube were the same as that in the experiment. A rigid piston was placed at the top surface with a displacement-controlled motion, and the bottom of the tube was clamped rigidly. To simulate the behavior of the NFM liquid, a phenomenological approach was taken: the tube was first filled with a liquid with the bulk modulus of 2.1 GPa, the same as that of water; upon loading, the pressure of the liquid quickly increased to 18 MPa, at which infiltration and the cell-wall buckling started. Using the pressure-volume curve of the NMF liquid measured earlier,[4] during the numerical simulation, the effective bulk modulus of the liquid filler was adjusted to decrease as a function of the cell volume. Finally, from both the force and the displacement acting on the piston, the relationship between the nominal stress and strain was computed, as shown in Fig. 3. It can be seen that the simulation has qualitatively captured the buckling initiation condition of the pressurized cell. The calculated critical nominal stress at the onset of cell-wall bucking is about 40 MPa, in good agreement with the experimental data. In terms of the buckled shape, the NFM liquid filled cell wrinkles and folds outward, and thus the wrinkle pattern is quite regular, whereas the empty cell may fold inward, and the pattern is relatively jerky, fitting well with the experimental observations (see Fig. 4). Note that, prior to the buckling,

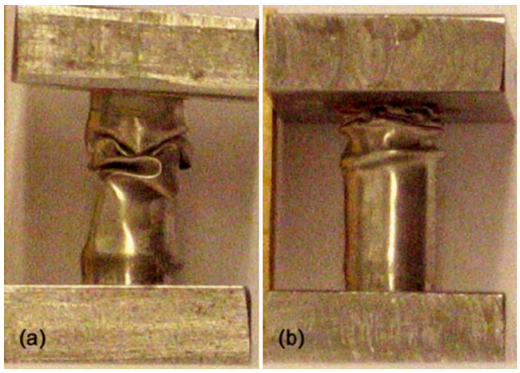

FIG. 4. (Color online) Photos of (a) a buckled empty cell and (b) a buckled NMF liquid enhanced cell. The initial outer diameter of the cell is 6.86 mm.

the extended yielding of tube wall occurs along the radius direction. If this effect was ignored, the calculated buckling stress and wrinkle size would be much larger than the experimental measurements. Due to the oversimplification of the boundary conditions and the material properties, the relaxation valley *CD* as well as the second increase in load in Fig. 2 cannot be simulated.

More detailed study on the rate dependence of the NMF liquid and its interactions with cell wall must be carried out to more accurately characterize the system performance. Systems containing multiple cells also need to be investigated so that the data can be directly relevant to honeycomb panels. Nevertheless, the experimental data and the numerical simulation have provided a proof-of-concept result that the energy absorption efficiency of a honeycomb can be improved by using nanoporous material functionalized liquids. The energy absorption is achieved via cell-wall buckling, extended yielding, as well as pressure-induced infiltration. The buckling process is highly nonuniform.

The experimental work was supported by The Army Research Office under Grant No. W911NF-05-1-0288. The numerical simulation was supported by the National Science Foundation under Grant No. NSF-CMS0407743.

[1]G. Lu and T. Yu, *Energy Absorption of Structures and Materials* (CRC, Boca Raton, FL, 2003).
[2]C. Z. Rosen, B. V. Hiremath, and R. E. Newnham, *Piezoelectricity* (American Institute of Physics, New York, 1992).
[3]X. Kong and Y. Qiao, Philos. Mag. Lett. **85**, 331 (2005).
[4]X. Kong and Y. Qiao, Appl. Phys. Lett. **86**, 151919 (2005).
[5]F. B. Surani, X. Kong, D. B. Panchal, and Y. Qiao, Appl. Phys. Lett. **87**, 163111 (2005).
[6]F. B. Surani, X. Kong, and Y. Qiao, Appl. Phys. Lett. **87**, 251906 (2005).
[7]L. J. Gibson and M. F. Ashby, *Cellular Solids: Structure and Properties* (Cambridge University Press, New York, 1997).
[8]D. Weaire and S. Hutzler, *The Physics of Foams* (Oxford University Press, New York, 1999).
[9]M. F. Ashby, A. G. Evans, N. A. Fleck, L. J. Gibson, J. W. Hutchinson, and H. N. G. Wadley, *Metal Foams: A Design Guide* (Elsevier Science, Burlington, MA, 2000).
[10]L. J. Gibson, MRS Bull. **28**, 270 (2003).
[11]O. Coussy, *Poromechanics* (Wiley, New York, 2004).
[12]X. Kong, F. B. Surani, and Y. Qiao, J. Mater. Res. **20**, 1042 (2005).
[13]F. B. Surani and Y. Qiao, J. Mater. Res. **21**, 1327 (2006).
[14]F. B. Surani and Y. Qiao, Mater. Res. Innovations **10**, 129 (2006).